



**Light assisted solar fuel production by artificial CO<sub>2</sub> Reduction and water Oxidation**

**Deliverable D2.2**

Report on iron and cobalt molecular catalysts active for the CO<sub>2</sub>R from CO<sub>2</sub> to CO

|                      |                                |
|----------------------|--------------------------------|
| Lead Beneficiary:    | ICIQ                           |
| Work Package:        | WP2                            |
| Delivery date:       | August 31 <sup>st</sup> , 2021 |
| Dissemination level: | Public                         |
| Version:             | 1.0                            |



This Project has received funding from the European Union's Horizon 2020 research and innovation program under grant agreement No. 951843

## D2.1. Nanocatalysts for CO<sub>2</sub>R

### Document Information

|                                  |   |
|----------------------------------|---|
| Grant Agreement Number           | 951843  |
| Acronym                          | LICROX  |
| Start date of project (Duration) | 01/09/2020 (36 months)  |
| Document due date                | 31/08/2021  |
| Submission date                  | 26/08/2021  |
| Authors                          | Antoni Llobet   |
| Deliverable number               | D2.2  |
| Deliverable name                 | Iron and cobalt molecular catalysts active for the CO <sub>2</sub> R from CO <sub>2</sub> to CO |
| WP                               | WP2 – CO <sub>2</sub> R tandem catalysis and WOC  |

| Version | Date       | Author               | Description                         |
|---------|------------|----------------------|-------------------------------------|
| v.0     | 09/08/2021 | Antoni Llobet (ICIQ) | Creation of the first draft         |
| v.1     | 25/08/2021 | Laura Villar (ICIQ)  | Revision, minor typo errors changed |

## EXECUTIVE SUMMARY

This document is a public report that contains information about molecular Fe and Co complexes containing porphyrin type of ligands that behave as powerful CO<sub>2</sub> reduction catalysts and that are labeled as Fe-P and Co-P respectively. Given the confidential nature of the work developed here we will describe only the redox and catalytic properties of the Fe-TPP (TPP is *meso*-tetraphenylporphyrin). The rest of the Fe-P behave in a similar manner but allowing to tune the onset of the catalytic waves as well the relative current densities at a particular potential. It is a deliverable of the LICROX Project, which is funded by the European Union's H2020 Program under Grant Agreement No. 951843. The best molecular Fe and Co CO<sub>2</sub> reduction catalysts described here will be later on anchored on solid supports in order to achieve heterogenous CO<sub>2</sub> reduction both alone and in combination with copper nanocrystals. Conductive and semiconductive solid supports will be used to achieve electro and photoelectrocatalysis respectively that will be ultimately integrated into a PEC for the generation of solar fuels.

## D2.1. Nanocatalysts for CO<sub>2</sub>R

### Table of Contents

|   |   |
|---|---|
| WP2: CO <sub>2</sub> R Tandem Catalysis and WOC .....                                 | 4 |
| 1. Purpose of the Nanocatalysts for CO <sub>2</sub> reduction .....                   | 4 |
| 2. Synthesis and characterization of the Fe-P and Co-P porphyrin complexes .....      | 4 |
| 3. Electrochemical characterization of Fe-P and Co-P in DMF in inert atmosphere ..... | 5 |
| 4. Electrocatalytic behavior of Fe-P and Co-P for the CO <sub>2</sub> R reaction..... | 5 |
| 5. Conclusions and future prospects .....   | 6 |
| 6. References .....   | 7 |

## D2.1. Nanocatalysts for CO<sub>2</sub>R

### WP2: CO<sub>2</sub>R Tandem Catalysis and WOC

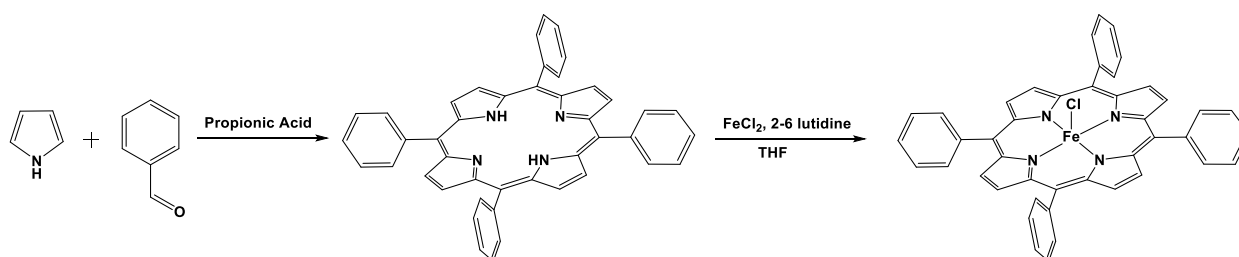
The role of WP2 is to implement the preparation of efficient catalysts that will perform the chemical reaction associated with the CO<sub>2</sub> reduction reaction (CO<sub>2</sub>RR) to yield solar fuels and in combination with the WOC to give oxygen gas in order to achieve high catalytic rates (high currents) and low working voltages.

#### 1. Purpose of the Nanocatalysts for CO<sub>2</sub> reduction

Molecular Fe and Co complexes containing porphyrin type of ligands are powerful CO<sub>2</sub> reduction catalysts. These complexes are synthetically highly versatile given the large number of substituents that the porphyrin type of ligands can tolerate. This results in a large family of porphyrin complexes with a precise control of the electronic and steric effects and even second coordination effects, that can be exerted over the Fe and Co metal centers. This in turn, is important since the metal center is where the key reactions occurs during the catalysis cycle including CO<sub>2</sub> coordination that normally is the rate determining step as well as multiple electron transfer events. As a consequence of all this, an exquisite control of the CO<sub>2</sub> reduction, overpotentials, turnover numbers, turnover frequencies and product distribution can be achieved with molecular Fe and Co porphyrin complexes depending of the solvent as well as the applied potential exerted over them. One of the main targets in this project will be to selectively form CO that can work in tandem with Cu nanocrystals in order to generate C<sub>1</sub> or C<sub>2+</sub> molecules. In addition, we will also target the efficient transformation of CO<sub>2</sub> directly to the mentioned C<sub>n</sub> products.

#### 2. Synthesis and characterization of the Fe-P and Co-P porphyrin complexes

There is a number of synthetic strategies that can be used for the preparation of porphyrin type of ligands. The most straight forward strategy consists on the reaction of pyrrole with an aldehyde as shown in the Scheme 1, below.<sup>1</sup> In most cases the purification of the final porphyrin as well as the synthetic intermediates involves the use of chromatography techniques. The proper characterization of porphyrin ligands involves the use of NMR spectroscopy as can be shown in Figure 1, left.



**Scheme 1.** Synthetic strategy for the preparation of porphyrin ligands and their complexes

The interaction of a metal precursor such as Fe or Co chloride, triflate, acetate etc. generates the corresponding complex. A sufficiently good crystal of the [FeCl(TPP)] complex was obtained and single crystal XRD was carried out. The ORTEP plot of its molecular structure is shown in Figure 1, right. Further characterization of these complexes involved the typical analytic techniques, UV-vis and electrochemistry. The latter is presented in the following section.

## D2.1. Nanocatalysts for CO<sub>2</sub>R

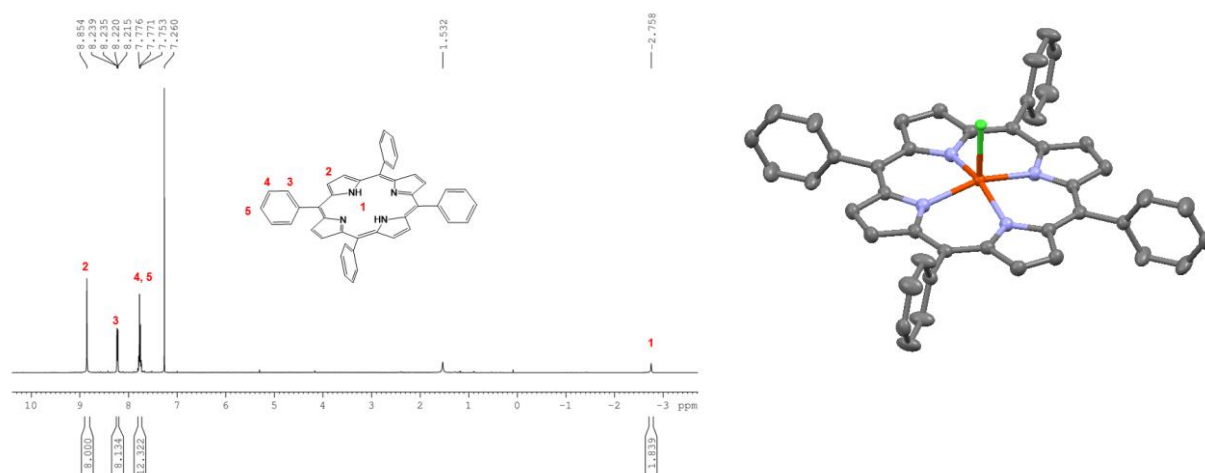


**Figure 1.** Left, <sup>1</sup>H-NMR of  $\text{H}_2\text{TPP}$  in  $\text{CDCl}_3$  with proton assignment. Right, Mercury plot of the crystal structure of  $[\text{FeCl}(\text{TPP})]$ . Color code: Ru, red; Cl, green; N, blue; C, gray. H atoms are omitted.

## 3. Electrochemical characterization of Fe-P and Co-P in DMF in inert atmosphere

The CO<sub>2</sub> reduction reaction as well as any redox reaction invariably involves electron transfer. For this reason, it is imperative to understand and control the degree of electron donation/withdrawing exerted by the ligands since this will influence the potentials where the redox events will occur.

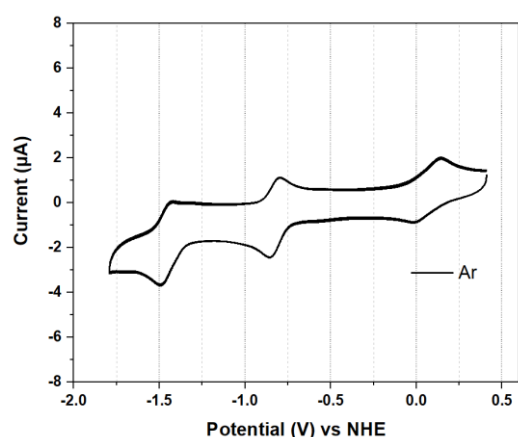


**Figure 2.** CV of  $[\text{FeCl}(\text{TPP})]$  in DMF under an inert atmosphere of Ar at 100 mV/s scan rate.

The electrochemical characterization was carried out by means of cyclic voltammetry (CV), differential pulse voltammetry (DPV) and bulk electrolysis (BE).

Figure 2 (black trace) shows the CV of  $[\text{FeCl}(\text{TPP})]$  in DMF in an Ar atmosphere. The first reduction appears at  $E_{1/2} = +0.07$  V vs. NHE and is associated with the  $\text{Fe}^{\text{III}}/\text{Fe}^{\text{II}}$  couple. The second and third reduction waves appear at -0.84 and -1.46 V vs. NHE and are associated with two consecutive one electron mainly ligand-based reductions.<sup>2,3</sup> However, for easy track of electron counting we will label them as if they were metal based as  $\text{Fe}^{\text{II}}/\text{Fe}^{\text{I}}$  and  $\text{Fe}^{\text{I}}/\text{Fe}^0$  respectively.

## 4. Electrocatalytic behavior of Fe-P and Co-P for the CO<sub>2</sub>R reaction

Figure 3 also shows the CV of Fe-TPP in the presence of CO<sub>2</sub> only (green trace) and in the presence of CO<sub>2</sub> and 1.0 M TFE that acts as proton source (blue line). As it can be observed in the presence of only CO<sub>2</sub> (green trace), the second reduction wave associated with the  $\text{Fe}^{\text{I}}/\text{Fe}^0$  couple increases substantially and its current density nearly doubles indicating the presence of CO<sub>2</sub> reduction catalysis. In sharp contrast in the presence of TFE as a proton source (blue trace), the intensity of the catalytic wave increases dramatically up to 300  $\mu\text{A}/\text{cm}^2$  indicating the presence of a highly efficient CO<sub>2</sub> reduction process. It is interesting to observe

## D2.1. Nanocatalysts for CO<sub>2</sub>R

the differences between the first and second cycles of these CVs under CO<sub>2</sub> and TFE. On the second cycle the initial Fe<sup>II</sup>/Fe<sup>I</sup> wave has completely disappeared from the double layer due to the formation of Fe<sup>I</sup>-CO complex (because of the large amount of CO generated in the first cycle at the double layer) whose redox wave appears at  $E_{1/2} = -1.05$  V ( $E_{p,c} = -1.08$  V;  $E_{p,a} = -1.02$  V). This assignment is corroborated by running a CV in the presence of CO instead of CO<sub>2</sub>. Further scanning on the reduction side replicates the electrocatalytic current density observed in the first cycle which indicates that at this potential the [Fe<sup>I</sup>(CO)(TPP)]- complex is quickly reduced to Fe<sup>0</sup> reentering the original catalytic cycle.

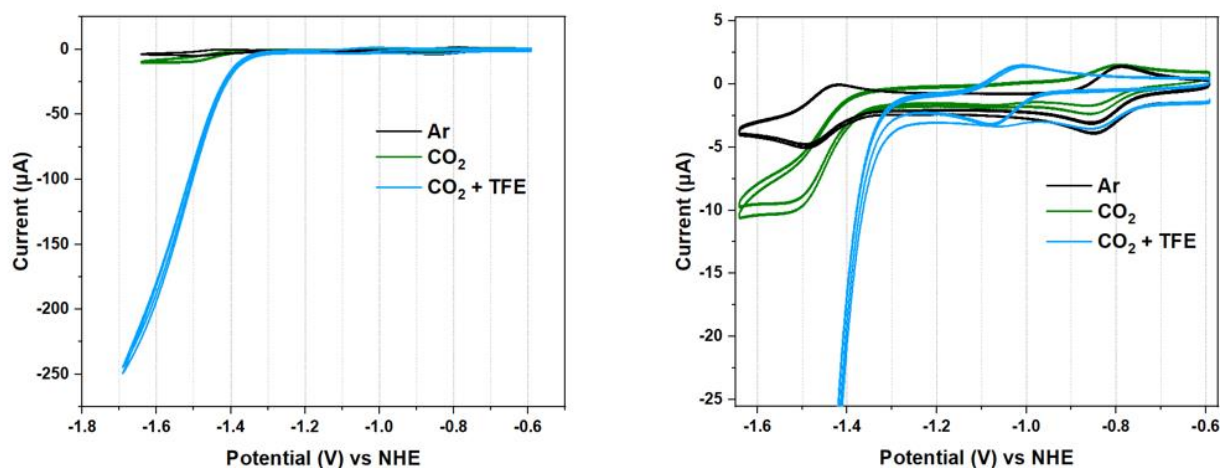


**Figure 3.** Left, CV of [FeCl(TPP)] in DMF under an inert atmosphere (black trace), in the presence of 1 atm of CO<sub>2</sub> (green trace) and under 1atm of CO<sub>2</sub> and 1.0 M TFE (blue trace) at a scan rate of 100 mV/s. Right, an enlargement of the -(0-25) μA zone.

Further, bulk electrolysis experiments for the [FeCl(TPP)] catalyst were carried out at an  $E_{app} = -1.6$  V for 1 h using a Glassy Carbon rod as a working electrode with a surface area of 1.23 cm<sup>2</sup> (Charge: -4.08 Q, Electrons:  $4.0 \times 10^{-5}$  mols). The major product detected is CO (95%) with very small amounts of H<sub>2</sub> (<1%). We also carried out the electrochemistry corresponding Co-TPP complex in order to check its catalytic properties. However, its performance is worse than the corresponding Fe-TPP and thus, we decided to focus our attention on the Fe complexes.

## 5. Conclusions and future prospects

The work described up to now is based mainly on the Fe-TPP complex that is used as a reference for this work. This already achieves current densities in the range of 3 mA/cm<sup>2</sup> at 1.8 V in DMF. The next step consists on using all the knowledge gained here and anchored these Fe-P catalysts on solid supports. The anchored catalyst will have a large amount of sample per surface area, and thus current densities are expected to increase by more than one order of magnitude with regard to the ones reported in homogeneous phase. Further the system will be probed in aqueous solution at pH 7, that is needed to be able to properly assemble it into the final PEC. In water the onset of the catalytic wave is expected to shift anodically by approx. 400 mV. All things considered this family of Fe-P developed so far has the right electrochemical properties needed to achieve the 10 mA/cm<sup>2</sup> at 300 mV overpotential. A second goal will consist on using the Fe-P with the right  $E_{1/2}$  for the Fe<sup>0</sup>/Fe<sup>I</sup> couple, so that it can provide a sufficiently high concentration of CO to the Cu nanocrystals at their best working potential, for the formation of C<sub>n</sub> products out of CO.

## D2.1. Nanocatalysts for CO<sub>2</sub>R

### 6. References

1. Costentin, C.; Robert, M.; Savéant, J.-M., *Acc. Chem. Res.*, **2015**, *48*, 2996.
2. Davethu, P.A.; de Visser, S.P., *J. Phys. Chem. A*, **2019**, *123*, 6527.
3. Römelt, C.; Ye, S.; Bill, E.; Weyhermüller, T.; van Gastel, M.; Neese, F., *Inorg. Chem.*, **2018**, *57*, 2141.